Discontinuous Optical Flow: Recent Theoretical Results

S. S. Beauchemin[†§] A. Chalifour[†] J. L. Barron[§]

† Université du Québec à Trois-Rivières
C.P. 500, Trois-Rivieres, Canada
G9A 5H7

§ The University of Western Ontario
London, Canada
N6A 5B7

Abstract

We present a theory of occlusion in the context of optical flow computation. In this contribution we derive, under models of constant and linear optical flow, several propositions describing the frequency structure of motion discontinuities arising from occlusion events in the spatial domain. We show that a wealth of crucial information is most easily obtainable from the analysis of the structure of occlusion in Fourier space. For instance, the identification of the occluding and occluded velocities is possible. We also demonstrate the geometrical properties of degenerate cases occurring when signals suffer from the aperture problem. In particular, we show that the full velocity of a degenerate occluding signal is almost always obtainable at the occlusion. We conclude by showing that additive translucency phenomena may be reduced to special cases of the theory.

1 Introduction

Traditionally, image motion and its approximation known as optical flow have been treated as continuous functions of the image domain [4]. However, in realistic imagery, one exceedingly rarely finds cases verifying this hypothesis. Many phenomena may cause discontinuities in the optical flow function of imagery [6]. Among them, occlusion and translucency are frequent causes of discontinuities in realistic imagery. In addition, their information content is useful to later stages of processing [2] such as motion segmentation [1] and 3-d surface reconstruction [7].

Occlusion boundaries are described as the partial occlusion of a surface by another, while translucency is defined as occlusion of a surface by translucent material. In realistic imagery, one finds occlusion to be the most frequent cause of discontinuous motion.

In this contribution, we investigate the structure of occlusion and transparency in the Fourier domain. Our motivation comes from the fact that the very presence of occlusions or surface translucence renders the usage of usual methods such as differentiation and region matching very difficult. Further, we postulate that spatial information constitutes an obstacle to determining discontinuous optical flow caused by occlusion. We derive, under models of constant and linear optical flow, several propositions describing the structure of motion discontinuities in Fourier space, arising from occlusion events in the spatial domain. We show that a wealth of crucial information is most easily obtainable from the analysis of the structure of occlusion in Fourier space. For instance, the identification of the occluding and occluded velocities is possible. We also demonstrate the geometrical properties of degenerate cases occurring when signals suffer from the aperture problem. In particular, we show that the full velocity of an occluding signal suffering from the aperture problem is almost always obtainable. We conclude by showing that additive translucency phenomena may be reduced to special cases of the theory.

2 Multiple Motions

Given an arbitrary environment and a moving visual sensor, the motion field generated onto the imaging plane by a 3-d scene within the visual field is represented as a function of the motion parameters of the visual sensor, usually expressed as instantaneous translation $\mathbf{T} = (T_x, T_y, T_z)^T$ and rotation $\mathbf{\Omega} = (\Omega_x, \Omega_y, \Omega_z)^T$:

$$\mathbf{v} = \begin{pmatrix} Z(\mathbf{x})^{-1}(xT_z - T_x) \\ Z(\mathbf{x})^{-1}(yT_z - T_y) \end{pmatrix} + \begin{pmatrix} xy\Omega_x - (1+x^2)\Omega_y + y\Omega_z \\ (1+y^2)\Omega_x - xy\Omega_y - x\Omega_z \end{pmatrix}, \quad (1)$$

where $\mathbf{x} = (x, y)^T$ is the perspective projection of a point $\mathbf{P}^T = (X, Y, Z)$ in the visual field. Assuming that the motion of the visual sensor is continuous (that is to say: $\mathbf{\Omega}$ and $\mathbf{T}$ are differentiable with respect to time), discontinuities in image motion are then introduced in (1) whenever the depth function $Z(\mathbf{x})$ is other than single-valued and differentiable. The occurrence of occlusion causes the depth function to exhibit a discontinuity, whereas translucency leads to a multiple-valued depth function.

Towards a useful generalization of this analysis, we show the structure of occlusion in Fourier space for one and two-dimensional signals and various models of optical flow. For instance, we consider constant and linear models of the optical flow function in both 1 and 2D. We also explore degenerate cases in which

either one or both the occluding and occluded signals suffer from the aperture problem[1].

2.1 Models of Optical Flow

The optical flow function may be expressed as an order n function of the image coordinates. Generally, we may write the Taylor series expansion for a ith velocity as:

$$\mathbf{v}_i^{(n)}(\mathbf{x},t) = \sum_{j=0}^{p}\sum_{k=0}^{q} \frac{\partial^{j+k}\mathbf{v}_i(\mathbf{x})}{j!k!\partial x^j \partial y^k} x^j y^k - \mathbf{a}_i t \quad p+q \leq n \tag{2}$$

where $\mathbf{a}_i t$ is the translational component. For instance, expansions of order $n = 0,1$ and 2 may be written out in full as:

$$\mathbf{v}_i^{(0)}(\mathbf{x},t) = \mathbf{x} - \mathbf{a}_i t \tag{3}$$

$$\mathbf{v}_i^{(1)}(\mathbf{x},t) = J_i\mathbf{x} - \mathbf{a}_i t \tag{4}$$

$$\mathbf{v}_i^{(2)}(\mathbf{x},t) = J_i\mathbf{x} + \begin{pmatrix} \mathbf{x}^T H_i(u)\mathbf{x} \\ \mathbf{x}^T H_i(v)\mathbf{x} \end{pmatrix} - \mathbf{a}_i t \tag{5}$$

where J_i is the Jacobi matrix and $H_i(u)$ and $H_i(v)$ are Hessian matrices:

$$\mathbf{a}_i = \begin{pmatrix} a_{i6} \\ b_{i6} \end{pmatrix} \quad J_i = \begin{pmatrix} a_{i1} & a_{i2} \\ b_{i1} & b_{i2} \end{pmatrix}$$

$$H_i(u) = \begin{pmatrix} a_{i3} & a_{i5} \\ a_{i5} & a_{i4} \end{pmatrix} \quad H_i(v) = \begin{pmatrix} b_{i3} & b_{i5} \\ b_{i5} & b_{i4} \end{pmatrix}.$$

These three models of optical flow comprise most of the inherent structure of image motion. For instance, the image motion of a planar surface is given by a 2nd-Order model in which we observe the following relationship among derivatives:

$$a_{i3} = 2b_{i5} \quad b_{i3} = 0 \quad a_{i4} = 0 \quad b_{i4} = 2a_{i5}. \tag{6}$$

2.2 Occlusion in the Frequency Domain

Consider a signal $\mathbf{I}_i(\mathbf{x},t)$ translating at a constant (or 0th-Order) velocity $\mathbf{v}_i^{(0)}(\mathbf{x},t)$. For this signal, the Fourier transform of the optical flow constraint equation is obtained with the differentiation property as:

$$\mathcal{F}\left[\nabla\mathbf{I}_i(\mathbf{x},t)^T\mathbf{a}_i + \mathbf{I}_{it}\right] = i\hat{\mathbf{I}}_i(\mathbf{k},\omega)\delta(\mathbf{k}^T\mathbf{a}_i + \omega), \tag{7}$$

where i is the imaginary number, $\hat{\mathbf{I}}_i(\mathbf{k},\omega)$ is the Fourier transform of $\mathbf{I}_i(\mathbf{x},t)$ and $\delta(\mathbf{k}^T\mathbf{a}_i+\omega)$ is a Dirac delta function. Expression (7) yields $\mathbf{k}^T\mathbf{a}_i + \omega = 0$ as a constraint on velocity. Similarly, the Fourier transform of a translating intensity profile $\mathbf{I}_i(\mathbf{x},t)$ is obtained with the shift property as:

$$\begin{aligned} \hat{\mathbf{I}}(\mathbf{k},\omega) &= \int\int \mathbf{I}_i(\mathbf{v}_i^{(0)}(\mathbf{x},t))e^{-i(\mathbf{k}^T\mathbf{x}+\omega t)}d\mathbf{x}dt \\ &= \int\left[\int \mathbf{I}_i(\mathbf{v}_i^{(0)}(\mathbf{x},t))e^{-i\mathbf{k}^T\mathbf{x}}d\mathbf{x}\right]e^{-i\omega t}dt \\ &= \hat{\mathbf{I}}_i(\mathbf{k})\delta(\mathbf{k}^T\mathbf{a}_i + \omega), \end{aligned} \tag{8}$$

which also yields the constraint $\mathbf{k}^T\mathbf{a}_i + \omega = 0$. Hence, (7) and (8) demonstrate that the frequency analysis of image motion is in accordance with the motion constraint equation [2]. It is also observed that $\mathbf{k}^T\mathbf{a}_i + \omega = 0$ represents, in the frequency domain, an oriented plane passing through the origin, with normal vector $\mathbf{a}_i$ representing full velocity, onto which the Fourier spectrum of $\mathbf{I}_i(\mathbf{x})$ lies.

Following Fleet and Jepson [2], the discontinuities in optical flow arising from occlusion may be written by considering two translating intensity profiles, one partially occluding the other. Let $\mathbf{I}_1(\mathbf{x})$ and $\mathbf{I}_2(\mathbf{x})$ be the intensity profiles of an object and a background scene. An object indicator function such as

$$\mathbf{U}(\mathbf{x}) = \begin{cases} 1 & \text{if } \mathbf{I}_1(\mathbf{x}) \neq 0 \\ 0 & \text{otherwise} \end{cases}$$

may be defined to specify the actual location of the object on the image plane. The resulting intensity pattern is then written as a function of the intensity profiles of the object, the background and the object indicator:

$$\begin{aligned} \mathbf{I}(\mathbf{x},t) &= \mathbf{I}_1(\mathbf{v}_1^{(0)}(\mathbf{x},t)) \\ &+ \left[1 - \mathbf{U}(\mathbf{v}_1^{(0)}(\mathbf{x},t))\right]\mathbf{I}_2(\mathbf{v}_2^{(0)}(\mathbf{x},t)). \end{aligned} \tag{9}$$

By using the shift property of Fourier transforms, (9) is rewritten in spatiotemporal frequency space as:

$$\begin{aligned} \hat{\mathbf{I}}(\mathbf{k},\omega) = & \\ & \hat{\mathbf{I}}_1(\mathbf{k})\delta(\mathbf{a}_1^T\mathbf{k}+\omega) + \hat{\mathbf{I}}_2(\mathbf{k})\delta(\mathbf{a}_2^T\mathbf{k}+\omega) \\ - & \left[\hat{\mathbf{U}}(\mathbf{k})\delta(\mathbf{a}_1^T\mathbf{k}+\omega)\right] * \left[\hat{\mathbf{I}}_2(\mathbf{k})\delta(\mathbf{a}_2^T\mathbf{k}+\omega)\right]. \end{aligned} \tag{10}$$

The first two terms of (10) are the signals associated with the object and the background. The frequency spectra of $\mathbf{I}_1$ and $\mathbf{I}_2$ are located on the planes defined by the equations $\mathbf{k}^T\mathbf{a}_1 + \omega = 0$ and $\mathbf{k}^T\mathbf{a}_2 + \omega = 0$ respectively. In addition, the respective orientations of these planes fully determine $\mathbf{a}_1$ and $\mathbf{a}_2$. The last term of (10) describes the distortion created by the occlusion boundary. In the following sections, this form of distortion is analized for various optical flow models in one and two dimensions and its usefulness in determining image events giving rise to multiple motions is shown.

[1] The aperture problem arises when the Fourier spectrum of $\mathbf{I}_i(\mathbf{x})$ is concentrated on a line rather than on a plane [2, 5]. Spatiotemporally, this depicts the situation in which $\mathbf{I}_i(\mathbf{x},t)$ exhibits a single spatial orientation. In this case, one only obtains the speed and direction of motion normal to the orientation, noted as $\mathbf{v}_{\perp i}(\mathbf{x},t)$. If many normal velocities are found in a single neighbourhood, their respective lines fit the plane $\mathbf{k}^T\mathbf{a}_i + \omega = 0$ from which full velocity may be obtained.

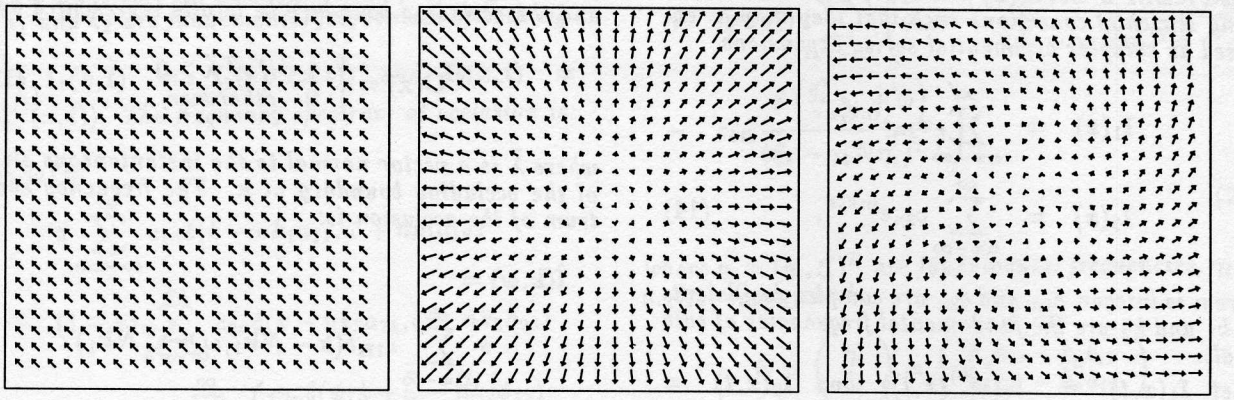

Figure 1: *Examples of constant and linear optical flow fields.* **a) (left):** *constant,* **b) (middle):** *dilational and* **c) (right):** *rotational.*

3 Occlusion with 0th-Order Models

In this section, we consider three cases of occlusion with velocities described as 0th-Order Taylor series expansions. The analysis begins with the consideration of a simple case consisting of two 1-d sinusoidal intensity profiles translating at constant velocities. The result is then generalized to arbitrary signals in one and two dimensions.

3.1 One Dimensional Sinusoidal Signals

The case in which two 1-d sinusoidals play the role of the object and the background is first considered. The 1-d version of the 0th-Order optical flow function (3) is written as $v_i^{(0)}(x,t) = x - a_{i6}t$. Let $\mathbf{I}_i(x)$ be a 1-d intensity function translating with velocity $\mathbf{v}_i^{(0)}(x,t)$ such that $\mathbf{I}_i(x,t) = \mathbf{I}_i(v_i^{(0)}(x,t))$. Its Fourier transform is $\hat{\mathbf{I}}_i(k,\omega) = \hat{\mathbf{I}}_i(k)\delta(ka_{i6}+\omega)$. Let $\mathbf{I}_1(x)$ be occluding another 1-d intensity pattern $\mathbf{I}_2(x)$, with respective velocities $v_1^{(0)}(x,t)$ and $v_2^{(0)}(x,t)$. The resulting intensity profile can then be expressed as:

$$\begin{aligned}\mathbf{I}(x,t) &= \mathbf{u}(v_1^{(0)}(x,t))\mathbf{I}_1(v_1^{(0)}(x,t)) \\ &+ (1-\mathbf{u}(v_1^{(0)}(x,t))) - \mathbf{I}_2(v_2^{(0)}(x,t))\end{aligned} \tag{11}$$

where $\mathbf{u}(x)$ is Heaviside's function representing the occluding point:

$$\mathbf{u}(x) = \begin{cases} 1 & \text{if } x \geq 0 \\ 0 & \text{otherwise.}\end{cases}$$

The Fourier transform of the intensity profile (11) is:

$$\begin{aligned}\hat{\mathbf{I}}(k,\omega) &= [\hat{\mathbf{u}}(k)\delta(ka_{16}+\omega)] * [\hat{\mathbf{I}}_1(k)\delta(ka_{16}+\omega)] \\ &- [\hat{\mathbf{u}}(k)\delta(ka_{16}+\omega)] * [\hat{\mathbf{I}}_2(k)\delta(ka_{26}+\omega)] \\ &+ \hat{\mathbf{I}}_2(k)\delta(ka_{26}+\omega),\end{aligned} \tag{12}$$

where $\hat{\mathbf{u}}(k)$ is the Fourier transform of Heaviside's function $\mathbf{u}(x)$ written as $\hat{\mathbf{u}}(k) = \pi\delta(k) + (ik)^{-1}$.

THEOREM 1 *Let $\mathbf{I}_1(x)$ and $\mathbf{I}_2(x)$ be cosine functions with respective angular frequencies $k_1 = 2\pi f_1 > 0$ and $k_2 = 2\pi f_2 > 0$ and let $\mathbf{I}_1(v_1^{(0)}(k_1x,t)) = c_1\cos(k_1x - a_{16}t)$ and $\mathbf{I}_2(v_2^{(0)}(k_2x,t)) = c_2\cos(k_2x - a_{26}t)$.*

The frequency spectrum of the occlusion is:

$$\begin{aligned}\hat{\mathbf{I}}(k,\omega) &= \frac{\pi}{2}c_1\delta(k\pm k_1, \omega\mp k_1a_{16}) \\ &+ \frac{(1-\pi)}{2}c_2\delta(k\pm k_2,\omega\mp k_2a_{26}) \\ &+ \frac{i}{2}\left(\frac{c_2\delta(ka_{16}+\omega\pm k_2\Delta a_6)}{(k\pm k_2)}\right. \\ &- \left.\frac{c_1\delta(ka_{16}+\omega)}{(k\pm k_1)}\right)\end{aligned} \tag{13}$$

where $\Delta a_6 = a_{16} - a_{26}$.

A number of conclusions can be drawn from Theorem 1: Since the signals are cosines, all their power content is real. In addition, the power content of the distortion term is entirely imaginary, and form lines of decreasing power about the frequencies of both the occluding and occluded signals. Their orientation is proportional to the velocity of the occluding signal, as $-a_{16}$ is the slope of the constraint lines. Hence, the distortion terms form lines parallel to the constraint line of the occluding signal.

3.2 One Dimensional Arbitrary Signals

In general, the occluding and occluded signals cannot be represented as simple sinusoidal functions. To gain generality, $\mathbf{I}_1(x)$ and $\mathbf{I}_2(x)$ may be expanded as complex exponential expansions, assuming that functions $\mathbf{I}_1(x)$ and $\mathbf{I}_2(x)$ satisfy Dirichlet conditions [3].

THEOREM 2 *Let $\mathbf{I}_1(x)$ and $\mathbf{I}_2(x)$ be functions satisfying Dirichlet conditions such that they may be expressed as complex exponential series expansions:*

$$\begin{aligned} \mathbf{I}_1(x) &= \sum_{n=-\infty}^{\infty} c_{1n} e^{ink_1 x} \\ \mathbf{I}_2(x) &= \sum_{n=-\infty}^{\infty} c_{2n} e^{ink_2 x}, \end{aligned} \tag{14}$$

where n is integer, c_{1n} and c_{2n} are complex coefficients and k_1 and k_2 are the fundamental frequencies of both signals.

Let $\mathbf{I}_1(x,t) = \mathbf{I}_1(v_1^{(0)}(x,t))$ and $\mathbf{I}_2(x,t) = \mathbf{I}_2(v_2^{(0)}(x,t))$. The frequency spectrum of the occlusion is:

$$\begin{aligned} \hat{\mathbf{I}}(k,\omega) &= \pi \sum_{n=\infty}^{\infty} c_{1n}\delta(k - nk_1, \omega + nk_1 a_{16}) \\ &+ (1-\pi) \sum_{n=-\infty}^{\infty} c_{2n}\delta(k - nk_2, \omega + nk_2 a_{26}) \\ &+ i \sum_{n=-\infty}^{\infty} \left(\frac{c_{2n}\delta(ka_{16} + \omega - nk_2 \Delta a_6)}{(k - nk_2)} \right. \\ &- \left. \frac{c_{1n}\delta(ka_{16} + \omega)}{(k - nk_1)} \right). \end{aligned} \tag{15}$$

Theorem 2 is an important generalization of the first one: Any signal which represents a physical quantity satisfies Dirichlet conditions and therefore may be expressed as an expansion of complex exponentials. Since c_{1n} and c_{2n} are complex coefficients, the power contents of the signals are both real and imaginary.

3.3 Two Dimensional Arbitrary Signals

Imagery is the result of the projection of light reflected by environmental features onto the imaging plane of the visual sensor. Hence, such signals are inherently two dimensional. Towards a generalization of (15), (14) is expanded as series of 2-d complex exponentials.

THEOREM 3 *Let $\mathbf{I}_1(\mathbf{x})$ and $\mathbf{I}_2(\mathbf{x})$ be 2-d functions satisfying Dirichlet conditions such that they may be expressed as complex exponential series expansions:*

$$\begin{aligned} \mathbf{I}_1(\mathbf{x}) &= \sum_{\mathbf{n}=-\infty}^{\infty} c_{1\mathbf{n}} e^{i\mathbf{x}^T N \mathbf{k}_1} \\ \mathbf{I}_2(\mathbf{x}) &= \sum_{\mathbf{n}=-\infty}^{\infty} c_{2\mathbf{n}} e^{i\mathbf{x}^T N \mathbf{k}_2}, \end{aligned} \tag{16}$$

where $\mathbf{n} = (n_x, n_y)^T$ and $N = \mathbf{n}^T I$ are integers, $\mathbf{x}$ are spatial coordinates, $\mathbf{k}_1 = (k_{1x}, k_{1y})^T$ and $\mathbf{k}_2 = (k_{2x}, k_{2y})^T$ are fundamental frequencies and $c_{1\mathbf{n}}$ and $c_{2\mathbf{n}}$ are complex coefficients.

Let $\mathbf{I}_1(\mathbf{x},t) = \mathbf{I}_1(\mathbf{v}_1^{(0)}(\mathbf{x},t))$, $\mathbf{I}_2(\mathbf{x},t) = \mathbf{I}_2(\mathbf{v}_2^{(0)}(\mathbf{x},t))$ and the occluding boundary be locally represented by:

$$\mathbf{U}(\mathbf{x}) = \begin{cases} 1 & \text{if } \mathbf{x}^T \vec{\lambda} \geq 0 \\ 0 & \text{otherwise,} \end{cases} \tag{17}$$

where $\vec{\lambda}$ is a vector normal to the instantaneous slope of the occluding boundary at $\mathbf{x}$. The frequency spectrum of the occlusion is:

$$\begin{aligned} &\hat{\mathbf{I}}(\mathbf{k},\omega) = \\ &\pi \sum_{\mathbf{n}=-\infty}^{\infty} c_{1\mathbf{n}}\delta(\mathbf{k} - N\mathbf{k}_1, \omega + \mathbf{a}_1^T N \mathbf{k}_1) \\ &+ (1-\pi) \sum_{\mathbf{n}=-\infty}^{\infty} c_{2\mathbf{n}}\delta(\mathbf{k} - N\mathbf{k}_2, \omega + \mathbf{a}_2^T N \mathbf{k}_2) \\ &+ i \sum_{\mathbf{n}=-\infty}^{\infty} \left(\frac{c_{2\mathbf{n}}\delta(\mathbf{k}^T \mathbf{a}_1 + \omega - \Delta \mathbf{a}_6^T N \mathbf{k}_2)}{(\mathbf{k} - N\mathbf{k}_2)^T \vec{\lambda}} \right. \\ &- \left. \frac{c_{1\mathbf{n}}\delta(\mathbf{k}^T \mathbf{a}_1 + \omega)}{(\mathbf{k} - N\mathbf{k}_1)^T \vec{\lambda}} \right). \end{aligned} \tag{18}$$

where $\Delta \mathbf{a}_6 = \mathbf{a}_1 - \mathbf{a}_2$.

Theorem 3 is a direct extension of Theorem 2 in two spatial dimensions. For this case, the constraint lines of previous Theorems 1 and 2 generated by both the occluding and occluded signals and the distortion terms become constraint planes. The frequency structure of each signal is preserved to within a scaling factor.

4 Occlusion with 1st-Order Models

The definition of optical flow as a constant model is limited. To gain generality, we develop propositions which express the structure of occlusion in the Fourier domain using linear models of optical flow. We use the 1st-Order expansion of (2), expressed as $\mathbf{v}_i^{(1)}(\mathbf{x},t) = \mathbf{x}^T J_i - \mathbf{a}_i t$. This linear model accounts for translation, rotation and dilation of the optical flow field.

4.1 One Dimensional Arbitrary Signals

In the case of one-dimensional signals, the optical flow function (4) reduces to the form $v_i^{(1)}(x,t) = a_{i1}x - a_{i6}t$. Thus, in one dimension, only dilation and translation exist.

THEOREM 4 *Let $\mathbf{I}_1(a_{11}x)$ and $\mathbf{I}_2(a_{21}x)$ be functions staisfying Dirichlet conditions such that they may be expressed as complex exponential series expansions:*

$$\begin{aligned} \mathbf{I}_1(a_{11}x) &= \sum_{n=-\infty}^{\infty} c_{1n} e^{ink_1 a_{11} x} \\ \mathbf{I}_2(a_{21}x) &= \sum_{n=-\infty}^{\infty} c_{2n} e^{ink_2 a_{21} x}, \end{aligned} \tag{19}$$

where n is integer, c_{1n} and c_{2n} are complex coefficients and k_1 and k_2 are fundamental frequencies of both signals.

Let $\mathbf{I}_1(x,t) = \mathbf{I}_1(v_1^{(1)}(x,t))$ *and* $\mathbf{I}_2(x,t) = \mathbf{I}_2(v_2^{(1)}(x,t))$. *The frequency spectrum of occlusion is:*

$$\begin{aligned}\hat{\mathbf{I}}(k,\omega) = & \\ & \pi \sum_{n=-\infty}^{\infty} c_{1n}\delta(k - nk_1a_{11}, \omega + nk_1a_{16}) \\ + & (1-\pi) \sum_{n=-\infty}^{\infty} c_{2n}\delta(k - nk_2a_{21}, \omega + nk_2a_{26}) \\ + & sgn(a_{11})\, i \sum_{n=-\infty}^{\infty} \left(\frac{c_{2n}\delta(\psi_1 k + \omega - nk_2\phi_{12})}{(k - nk_2a_{21})} \right. \\ - & \left. \frac{c_{1n}\delta(\psi_1 k + \omega)}{(k - nk_1a_{11})} \right) \end{aligned} \tag{20}$$

where

$$\psi_i = \frac{a_{i6}}{a_{i1}} \quad \text{and} \quad \phi_{ij} = \frac{a_{j1}a_{i6} - a_{i1}a_{j6}}{a_{i1}}$$

4.2 Two Dimensional Arbitrary Signals

The generalization of Theorem 4 to two dimensions defines the structure of occlusion under linear deformation. Therefore, the optical flow may exhibit translation, rotation, and dilation.

THEOREM 5 *Let* $\mathbf{I}_1(J_1\mathbf{x})$ *and* $\mathbf{I}_2(J_2\mathbf{x})$ *be 2-d functions satisfying Dirichlet conditions such that they may be expressed as complex exponential series expansions:*

$$\begin{aligned}\mathbf{I}_1(J_1\mathbf{x}) &= \sum_{\mathbf{n}=-\infty}^{\mathbf{n}=\infty} c_{1\mathbf{n}} e^{i\mathbf{k}^T N J_1 \mathbf{x}} \\ \mathbf{I}_2(J_2\mathbf{x}) &= \sum_{\mathbf{n}=-\infty}^{\mathbf{n}=\infty} c_{1\mathbf{n}} e^{i\mathbf{k}^T N J_2 \mathbf{x}} \end{aligned} \tag{21}$$

Let $\mathbf{I}_1(\mathbf{x},t) = \mathbf{I}_1(\mathbf{v}_1^{(1)}(\mathbf{x},t))$, $\mathbf{I}_2(\mathbf{x},t) = \mathbf{I}_2(\mathbf{v}_2^{(1)}(\mathbf{x},t))$ *and the occluding boundary be locally represented by:*

$$\mathbf{U}(J_1\mathbf{x}) = \begin{cases} 1 & \text{if } \vec{\lambda}^T J_1\mathbf{x} \geq 0 \\ 0 & \text{otherwise,} \end{cases} \tag{22}$$

where $\vec{\lambda}$ *is a vector normal to the instantaneous slope of the occluding boundary at* $J_1\mathbf{x}$. *The frequency spectrum of the occlusion is:*

$$\begin{aligned}\hat{\mathbf{I}}(\vec{\eta},\omega) = & \\ & \pi \sum_{\mathbf{n}=-\infty}^{\infty} c_{1\mathbf{n}}\delta(\vec{\eta}_1 - \gamma_1 N\vec{\eta}_1', \omega + \mathbf{a}_1^T N\vec{\eta}_1') \\ + & (1-\pi) \sum_{\mathbf{n}=-\infty}^{\infty} c_{2\mathbf{n}}\delta(\vec{\eta}_2 - \gamma_2 N\vec{\eta}_2', \omega + \mathbf{a}_2^T N\vec{\eta}_2') \\ + & sgn(\gamma_1)\, i \sum_{\mathbf{n}=-\infty}^{\infty} \left(c_{2\mathbf{n}} \frac{\delta\left(\frac{\vec{\eta}_1^T}{\gamma_1}\mathbf{a}_1 + \omega - \Delta\mathbf{a}_6^T N\vec{\eta}'_2\right)}{(\vec{\eta}_1 - \gamma_2 N\vec{\eta}_2')^T\vec{\lambda}} \right. \\ - & \left. c_{1\mathbf{n}} \frac{\delta\left(\frac{\vec{\eta}_1^T}{\gamma_1}\mathbf{a}_1 + \omega\right)}{(\vec{\eta}_1 - \gamma_1 N\vec{\eta}_1')^T\vec{\lambda}} \right) \end{aligned} \tag{23}$$

where $\vec{\eta}_i' = (\eta_i', \xi_i')^T$ *are fundamental frequencies,* $\gamma_i = a_{i1}b_{i2} - a_{i2}b_{i1}$ *and*

$$\vec{\eta}_i = \begin{pmatrix} \eta_i \\ \xi_i \end{pmatrix} = \begin{pmatrix} k_x b_{i2} - k_y b_{i1} \\ k_y a_{i1} - k_x a_{i2} \end{pmatrix}$$

Theorems 1 through 5 show the structure of occlusion in the Fourier domain for constant and linear models of optical flow in both 1 and 2D. These structures have interesting properties which we have informally outlined. We formally state them in form of geometrical theorems and corollaries.

COROLLARY 1 *Phenomena of additive translucency are special cases for which the distortion terms vanish in structural Theorems 1 through 5.*

In the case of an additive translucency phenomenon, there is no occlusion boundary associated with one of the signals and therefore no distortion terms in the Fourier structure are present. Hence, the spectrum of the translucency only exhibits the constraint planes of both signals, without distortion.

COROLLARY 2 *The structure of occlusion is invariant under 0th and 1st-Order models of optical flow.*

In both 1D and 2D cases, we find that the structural aspect of the Fourier spectrum is identical. The power generated by the distortion fits lines (or planes in 2D) that are parallel to the constraint line (or plane) of the occluding signal. Although the orientation of these structures depict ratios of the linear parameters, a collection of those in a neighbourhood yield these parameters in the least-squares sense. This result also indicates that we can use this structural invariance to accurately detect regions of occlusion under constant or linear optical flow with the same mechanism.

COROLLARY 3 *Under an occlusion phenomenon, the velocities of the occluding and occluded signals can always be identified as such.*

Under occlusion, the orientations of the distortion terms are essentially parallel to the constraint plane of the occluding signal. Hence, the orientation of the constraint plane containing the origin and parallel to the distortion terms yields the velocity of the occluding signal, thus associating the second velocity with the occluded signal.

5 The Aperture Problem: Degenerate Cases

The usual optical flow constraint equation, for a constant model of velocity, expressed as

$$\nabla \mathbf{I}_i(\mathbf{v}_i^{(0)}(\mathbf{x},t)) + \mathbf{I}_{it} = 0 \tag{24}$$

defines a single constraint on image motion. In Figure 2, normal velocity is defined as the vector from the origin perpendicular to the constraint line.

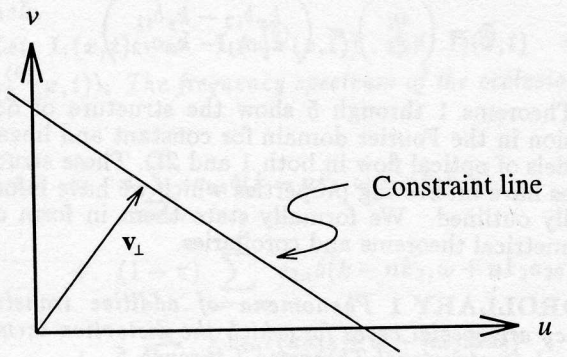

Figure 2: *The optical flow constraint equation defines a line in velocity space. The normal velocity* $\mathbf{v}_\perp$ *is defined as the vector perpendicular to the constraint line, i.e. the velocity with the smallest magnitude on the optical flow constraint line.*

Equation (24) is not sufficient to solve for both components of velocity. Only the velocity component in the direction of the local intensity gradient may be computed. This phenomenon is known as the *aperture problem* [8] and occurs when a given signal exhibits a unidimensional texture or, in other words, a unique local intensity gradient, which we term as a degeneracy (see Figure 3).

In the Fourier domain, the power spectrum of a degenerate signal is concentrated along a line rather than a plane. To see this, consider a 1D signal moving with a constant model of velocity in a 2D space, with velocity s_i along gradient normal $\mathbf{n}_i$:

$$\mathbf{I}(\mathbf{x},t) = \mathbf{I}_i(\mathbf{x}^T\mathbf{n}_i - s_i t) \tag{25}$$

The Fourier transform of this signal is given by

$$\hat{\mathbf{I}}(\mathbf{k},\omega) = \hat{\mathbf{I}}_i(\mathbf{k}^T\mathbf{n}_i)\delta(\mathbf{k}^T\mathbf{n}_i^\perp)\delta(s_i\mathbf{k}^T\mathbf{n}_i + \omega), \tag{26}$$

where $\mathbf{n}_i^\perp$ is the negative reciprocal of $\mathbf{n}_i$ [2]. The Dirac delta functions are both planar spectra and the intersection of these two planes form a 3D line onto which the spectrum of the degenerate signal resides. Therefore, the planar orientation describing full velocity is undetermined. However, the presence of an occlusion boundary disambiguates the measurement for the occluding signal in most cases.

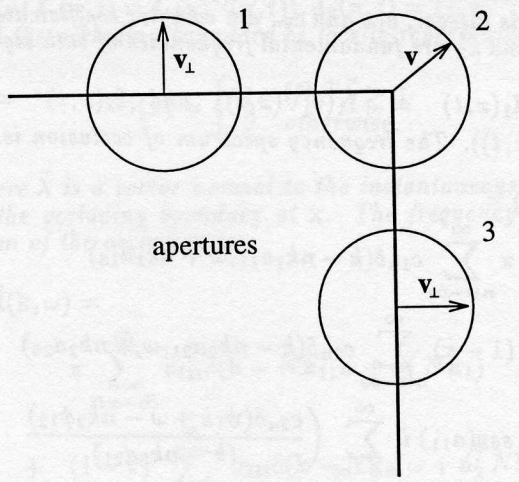

Figure 3: *Through apertures 1 and 3, only normal motions of the edges forming the square can be estimated, due to a lack of local structure. Inside aperture 2, at the corner point, the motion can be fully measured since there is sufficient local structure; both normal motions are visible.*

THEOREM 6 *The full velocity of a degenerate occluding signal in 2D is obtainable from the structure of the Fourier spectrum if and only if its normal is different from the normal of the occlusion boundary.*

An occlusion boundary, modeled as a locally straight ramp function, provides one constraint on component velocity. The degenerate signal also provides a second similar constraint. Since they are moving at the same full velocity, it is possible to solve the following system of equations

$$\begin{aligned} \frac{1}{\gamma_1}\left(\mathbf{a}_1^T\mathbf{n}_1 - s_1\right) &= 0 \\ \frac{1}{\gamma_1}\left(\mathbf{a}_1^T\mathbf{n}_2 - s_2\right) &= 0 \end{aligned} \tag{27}$$

leading to full velocity, as long as it is well conditioned, that is to say, that both normals and speeds are not identical. In the Fourier domain, the spectra of the degenerate signal and the occlusion boundary are both concentrated along lines with possibly different orientations, containing the origin. The orientation of the plane containing these two constraint lines yields a full velocity measurement.

THEOREM 7 *The case in which both the occluding and occluded signals are degenerate and the normals of the occluding signal and boundary are identical can be reduced to a 1D case of occlusion from which only normal velocities are obtainable.*

In this case, the constraint lines of the occluding signal and the occluding boundary are indistinguishable and form a single oriented line. The occluded

signal also provides such a line and, on the plane fitting these, the structure of the occlusion collapses to a 1D case.

6 Geometric Interpretation

We examine the geometrical properties of the Fourier spectra of constant and linear models of optical flow for both 1 and 2D signals.

6.1 0th-Order Models

In the simplest case involving sinusoidal signals, Theorem 1 shows that the frequency spectra of both signals are preserved to within scaling factors. In addition, the imaginary terms represent the frequency spectrum of the occlusion boundary. Figure 4 shows three cases of occlusion with 1D, Gaussian-windowed sinusoidal signals. The 1D velocities of the occluding signals are $a_{16} = -1.0$, -0.5 and 0.5 respectively. The velocities of the occluded signals are $a_{26} = -1.0$. The spatial frequency of the occluding and occluded signals are $k_1 = \frac{\pi}{8}$ and $k_2 = \frac{\pi}{16}$ respectively. The vertical axis represents temporal frequency ω while the horizontal axis is spatial frequency k. The spectral peaks located at $\pm(k_1, -k_1 a_{16})$ and $\pm(k_2, -k_2 a_{26})$ depict the spatiotemporal frequencies of both signals and fit the constraint lines $ka_{16} + \omega = 0$ and $ka_{26} + \omega = 0$. The oblique spectra intesecting the peaks represent the spectrum generated by the occlusion boundary and fit the constraint lines $k_1 a_{16} + \omega \pm k_2 a_{26} = 0$ and $k_1 a_{16} + \omega = 0$. These lines are parallel to the constraint line of the occluding signal. It also is interesting to observe from Theorem 2 that every non-zero frequency of an occluded signal shows such a parallel line due to occlusion.

Theorem 3 is the generalization of Theorem 2 in 2D and its geometric interpretation is similar. That is to say, the constraint lines of the signals and the occlusion boundary become constraint planes. For instance, the frequencies $(N\mathbf{k}_1, -\mathbf{a}_1^T N\mathbf{k}_1)$ and $(N\mathbf{k}_2, -\mathbf{a}_2^T N\mathbf{k}_2)$ fit the constraint planes of the occluding and occluded signals, defined as $\mathbf{k}_1^T\mathbf{a}_1 + \omega = 0$ and $\mathbf{k}^T\mathbf{a}_2 = 0$. In the distortion term, the arguments of the Dirac δ functions $\mathbf{k}^T\mathbf{a}_1 + \omega - \Delta\mathbf{a}_6^T N\mathbf{k}_2$ and $\mathbf{k}^T\mathbf{a}_1 + \omega$ represent a set of planes parallel to the constraint plane of the occluding signal $\mathbf{k}^T\mathbf{a}_1 + \omega = 0$. That is to say, for every discrete frequency $N\mathbf{k}_1$ and $N\mathbf{k}_2$ exhibited by both signals, there is a frequency spectrum fitting the planes given by $\mathbf{k}^T\mathbf{a}_1 + \omega - \Delta\mathbf{a}_6^T N\mathbf{k}_2 = 0$ and $\mathbf{k}^T\mathbf{a}_1 + \omega = 0$. The magnitudes of these planar spectra are determined by their corresponding scaling functions $c_{1\mathbf{n}}[(\mathbf{k} - N\mathbf{k}_1)^T\vec{\lambda}\,]^{-1}$ and $c_{2\mathbf{n}}[(\mathbf{k} - N\mathbf{k}_2)^T\vec{\lambda}\,]^{-1}$. Hence, Theorem 3 reveals useful constraint planes, as the power spectra of both signals peak within planes $\mathbf{k}^T\mathbf{a}_1 + \omega = 0$ and $\mathbf{k}^T\mathbf{a}_2 + \omega = 0$ and the constraint planes arising from the distortion are parallel to the spectrum of the occluding signal $\mathbf{I}_1(\mathbf{x}, t)$.

6.2 1st-Order Models

As a consequence of Corollary 2, the geometric interpretation of 1st-Order models of optical flow under occlusion is essentially similar to 0th-Order models. The difference lies in the interpretation of the quantities depicted by the orientations of the planar spectra representing the occluding and occluded signals. For instance, in Theorem 4, the orientations of these planar spectra represent ratios of the linear velocity parameters. These ratios are $\frac{a_{16}}{a_{11}}$ and $\frac{a_{26}}{a_{21}}$ for the occluding and occluded signals respectively. Such quantities are interpreted as the translation-to-scaling ratios of both signals. In the case of 2-d signals, as in Theorem 5, we find that the orientations of the planar spectra are proportional to the ratios $\frac{\vec{\eta}_1^T\mathbf{a}_1}{\gamma_1}$ and $\frac{\vec{\eta}_2^T\mathbf{a}_2}{\gamma_2}$ where γ_1 and γ_2 are the Jacobians of linear velocity matrices J_1 and J_2.

7 Conclusion

We have shown the Fourier structure of occlusion and translucency phenomena for constant and linear models of velocity in both 1 and 2D and shown various interesting geometrical properties. For instance, the constraint lines or planes cast by the occlusion boundary have been characterized. In a multiple motion situation, their presence indicates an occlusion while their absence indicates a translucency phenomenon.

When a multiple motion situation is caused by an occlusion, the parallelism between the the distortion cast by the occluding boundary and the Fourier spectrum of the occluding signal differentiates the velocity of the occluding signal from the velocity of the occluded signal. Further, this result holds for constant and linear models of optical flow.

The structural invariance of the Fourier structure of occlusion under constant and linear models of optical flow renders the accurate detection of regions exhibiting occlusion possible, whether the motions of the occluding or occluded surfaces are constant or linear.

In addition, the full velocity of a degenerate occluding signal is almost always obtainable. This result indicates that the information contained in the occlusion may be put to use to disambiguate velocity measurements.

Recovering the orientation of the Fourier structures does not lead to the recovery of the linear parameters of optical flow. However, a collection of these orientations from a neighbourhood yields the linear parameters in the least-squares sense.

Our current research following this analysis is the finding of the Fourier structure of 2nd-Order signals. Of particular importance is the Fourier structure of occluding planar surfaces in motion, which constitute a special case of 2nd-Order signals. In addition, a number of algorithms for detecting occlusion and transparency phenomena, identifying occluding and occluded velocities, and recovering occlusion boundaries are currently being developed.

Acknowledgements

We would like to thank P. K. Bose for meaningful discussions and comments. This research is supported by NSERC (National Science and Egineering Research Council of Canada).

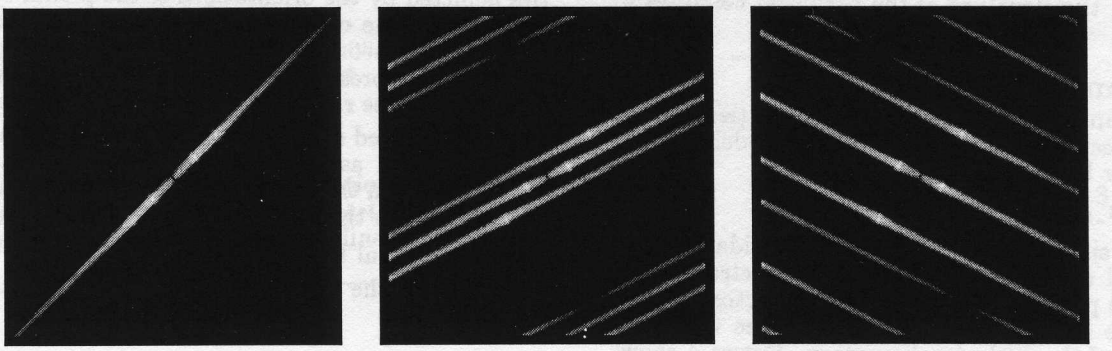

Figure 4: *Fourier spectra of occluding and occluded 1D sinusoids translating with various velocities, generated with Theorem 2.*

References

[1] G. Adiv. Determining three-dimensional motion and structure from optical flow generated by several moving objects. *IEEE PAMI*, 7(4):384–401, 1985.

[2] D. J. Fleet and A. D. Jepson. Computation of component image velocity from local phase information. *IJCV*, 5(1):77–104, 1990.

[3] J. D. Gaskill. *Linear Systems, Fourier Transforms and Optics.* Wiley & Sons, Inc., 1978.

[4] B. K. P. Horn and B. G. Schunck. Determining optical flow. *Artificial Intelligence*, 17:185–204, 1981.

[5] D. Marr and S. Ullman. Directional selectivity and its use in early visual processing. *Proceedings of Royal Society London*, B 211:151–180, 1981.

[6] M. Shizawa and K. Mase. Principle of superposition: A common computational framework for analysis of multiple motion. In *IEEE Proceedings of Workshop on Visual Motion*, pages 164–172, Princeton, New Jersey, October 1991.

[7] P. Toh and A. K. Forrest. Occlusion detection in early vision. In *ICCV*, pages 126–132. IEEE, 1990.

[8] S. Ullman. *The interpretation of visual motion.* MIT Press, Cambridge, London, 1979.